G.U. Journal of Science
23(1): 81-87 (2010)

GUJS
www.gujs.org

Comparison of the Linear Homing, Parabolic Homing and Proportional Navigation Guidance Methods on a Two-Part Homing Missile against a Surface Target

Bülent ÖZKAN [1♠], M. Kemal ÖZGÖREN [2], Gökmen MAHMUTYAZICIOĞLU [1]

[1] The Scientific and Technological Research Council of Turkey, Defense Industry Research and Development Institute (TÜBİTAK-SAGE), 06261, Ankara, Turkey
[2] Middle East Technical University, Faculty of Engineering, Mechanical Engineering Department, 06531, Ankara, Turkey

Received: 14.05.2009 Revised: 14.09.2009 Accepted: 29.09.2009

ABSTRACT

In this study, it is aimed at comparing the performance of the guidance methods called Linear Homing Guidance (LHG), Parabolic Homing Guidance (PHG), and Proportional Navigation Guidance (PNG) on a missile with two relatively rotating parts against a surface target. In this extent, first the dynamic model of the missile is constructed. Next, the guidance laws LHG, PHG, and PNG are formulated. Modelling the target kinematics as well, the entire guidance and control system is built by integrating all the models mentioned above, and the relevant computer simulations are carried out. Consequently, the simulation results are discussed and the study is evaluated.

Key Words: Guidance and Control, Two-part Missile, Linear Homing, Parabolic Homing, Proportional Navigation.

1. INTRODUCTION

Guided missiles have become one of the popular munitions in the military field because they have the ability of hitting the intended target precisely. This situation leads to the studies on the development of several guidance and control methods so as to increase the performance of the missiles [1]. In this sense, while the indirect guidance methods which mainly depend on the trajectory planning of the missile have been proposed against stationary targets, the direct guidance methods have been developed for moving targets [2, 3, 4]. The Linear Homing Guidance (LHG) and Parabolic Homing Guidance (PHG) methods handled in this study are in fact among the indirect guidance methods. On the other hand, the Proportional Navigation Guidance (PNG) law one of the widely-used direct guidance methods has become the most popular guidance law because of its simplicity and ease of implementation [2, 5, 6].

The success of a guided missile is dependent on certain factors. The most significant error sources affecting the success of a guided missile are the initial heading error of the missile and the target maneuvers. Apart from these, the dynamics of the guidance and control system, acceleration limit of the missile, mechanical limit of the aerodynamic control fins, and other external effects cause the missile to deviate from the target [2].

In this work, the entire guidance and control model is built for the two-part missile model considered and the performance of the missile is evaluated for the LHG, PHG, and PNG laws after adding the effects mentioned above to the model. Eventually, the results of the related computer simulations are submitted in a tabulated form.

2. DYNAMIC MODEL OF THE MISSILE

In this study, an aerodynamically-controlled canard-type missile consisting of two-bodies that are connected to each other by means of a roller bearing is dealt with. The equations of motion of the missile whose schematic

Corresponding author: bozkan@sage.tubitak.gov.tr

representation is given in Figure 1 can be obtained by applying the Newton-Euler force and moment equalities with respect to the body-fixed frame of the entire missile (F_b) in the following manner:

$$\dot{u} - r\,v + q\,w = (X + X_T)/m + g_x \quad (1)$$

$$\dot{v} + r\,u - p\,w = (Y + Y_T)/m + g_y \quad (2)$$

$$\dot{w} - q\,u + p\,v = (Z + Z_T)/m + g_z \quad (3)$$

$$\dot{p} = \left(L_1 + b_t\,\dot{\phi}_s\right)/I_{a1} \quad (4)$$

$$\dot{p}_2 = \left(L_2 + L_T - b_t\,\dot{\phi}_s\right)/I_{a2} \quad (5)$$

$$\dot{q} - p\,r\left(1 - (m_1/m_2)\right) + p_2\,r\left(I_{a2}/I_t\right) = \left(M + M_T - \lambda Z_T\right)/I_t \quad (6)$$

$$\dot{r} + p\,q\left(1 - (m_1/m_2)\right) - p_2\,q\left(I_{a2}/I_t\right) = \left(N + N_T + \lambda Y_T\right)/I_t \quad (7)$$

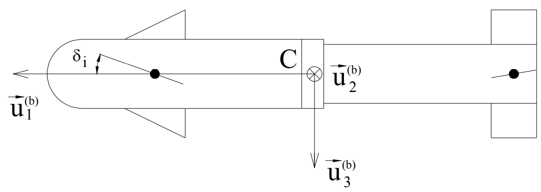

Figure 1. Missile model.

The parameters in equations (1) through (7) are defined as follows:

m, m_1, and m_2: Masses of the entire missile, front part, and rear part, respectively

I_{a1} and I_{a2}: Axial moment of inertia components of the front and rear bodies

I_t: Lateral moment of inertia component of the entire missile

b_t: Viscous friction coefficient of the roller bearing

λ: Distance between the mass centers of the entire missile and rear part

ϕ_s: Spin angle of the rear body about $\vec{u}_1^{(b)}$ axis

p, q, and r: Angular velocity components in the roll, pitch, and yaw directions

u, v, and w: Linear velocity components

X, Y, and Z: Aerodynamic force components acting on the missile at its mass centre (point C)

L_1 and L_2: Roll components of the aerodynamic moments acting on the front and rear parts

M and N: Pitch and yaw components of the aerodynamic moments acting on the missile body

X_T, Y_T, and Z_T: Thrust force components on the missile at its mass centre

L_T, M_T, and N_T: Thrust misalignment moment components

g_x, g_y, and g_z: Gravity components acting on the missile at its mass centre

As seen from equations (1) through (7), the two-part missile has an additional roll motion describing the roll motion of the rear body in equation (5) unlike a conventional single-part missile. On the other hand, this expression does not imply an extra control effort for the considered control scheme because it corresponds to an uncontrolled motion.

Supposing the roll motion of the missile, which is actually nothing but the roll motion of the front body carrying the guidance and control section of the missile, is compensated by means of a roll autopilot prior to the motions in the pitch and yaw directions, i.e. $p \approx 0$, the equations of motion of the missile in the pitch and yaw planes after the end of thrust can be written using equations (2), (3), (6), and (7) as follows:

$$\dot{w} - q\,u = (Z/m) + g_z \quad (8)$$

$$\dot{q} = M/I_t \quad (9)$$

$$\dot{v} + r\,u = (Y/m) + g_y \quad (10)$$

$$\dot{r} = N/I_t \quad (11)$$

3. AERODYNAMIC MODEL OF THE MISSILE

In the above expressions, the determination of the aerodynamic force and moment terms are the most challenging ones among the others. Many methods are available in the literature for introducing them [7, 8]. Here, the aerodynamic force and moment components in equations (8) through (11), i.e. Y, Z, M, and N, can be expressed in the following manner:

$$Y = C_y\,q_\infty\,S_M \quad (12)$$

$$Z = C_z\,q_\infty\,S_M \quad (13)$$

$$M = C_m\,q_\infty\,S_M\,d_M \quad (14)$$

$$N = C_n\,q_\infty\,S_M\,d_M \quad (15)$$

In equations (12) through (15), q_∞, S_M, and d_M stand for the dynamic pressure on the missile, missile cross-sectional area, and missile diameter, respectively. Regarding the considered missile geometry, the aerodynamic coefficients, i.e. C_y, C_z, C_m, and C_n, are computed for the Mach number, i.e. M_∞, in the range of 0.3 through 2.7, elevator and rudder deflections, i.e. δ_e and δ_r, in the range of −10 through 10°, and angle of attack and side-slip angle, i.e. α and β, in the range of −17 through 19°. Here, as a consistent approach, C_y, C_z, C_m, and C_n coefficients can be written in the form of linear functions of α, β, δ_e, δ_r, q, and r as given below:

$$C_y = C_{y_\beta}\,\beta + C_{y_\delta}\,\delta_r + C_{y_r}\,r\left(d_M/2v_M\right) \quad (16)$$

$$C_z = C_{z_\alpha}\,\alpha + C_{z_\delta}\,\delta_e + C_{z_q}\,q\left(d_M/2v_M\right) \quad (17)$$

$$C_m = C_{m_\alpha}\alpha + C_{m_\delta}\delta_e + C_{m_q}q(d_M/2v_M) \quad (18)$$

$$C_n = C_{n_\beta}\beta + C_{n_\delta}\delta_r + C_{n_r}r(d_M/2v_M) \quad (19)$$

In equations (16) through (19), v_M denotes the magnitude of the missile velocity vector. The stability derivatives represented by C_{y_β}, C_{y_δ}, C_{y_r}, C_{z_α}, C_{z_δ}, C_{z_q}, C_{m_α}, C_{m_δ}, C_{m_q}, C_{n_β}, C_{n_δ}, and C_{n_r} are functions of M_∞ and they are continuously updated depending on the present values of the related flight parameters during the computer simulations.

4. GUIDANCE LAWS

In this study, the terminal guidance phase which covers the duration from the instant at which the seeker detects the target to the end of the missile-target engagement is considered and the LHG, PHG, and PNG laws are employed in this phase in order to steer the missile toward the target. As introduced below in a more detailed manner, the LHG law yields guidance commands in terms of the flight path angles whereas PHG and PNG dictate commands to the lateral acceleration components of the missile. By the way, the commands of the PHG and PNG laws can also be expressed in the sense of the angular acceleration components of the missile [1].

4.1. Linear Homing Guidance Law

In this approach, it is intended to keep the missile always on the collision triangle that is formed by the missile, the target, and the predicted intercept point. For this purpose, the most appropriate way is to orient the missile velocity vector toward the predicted intercept point at which the missile-target collision will occur after a while as depicted in Figure 2. Then, the resulting guidance commands will be in the form of the flight path angles of the missile [1, 4, 9].

In Figure 2, O_e denotes the origin of the Earth-fixed frame; M, T, and P stand for the missile, the target, and the predicted intercept point, and $\vec{v}_{Mactual}$ and $\vec{v}_{Mideal}$ show the velocity vector of the missile at the beginning of the guidance and ideal velocity vector, respectively. The velocity vector of the missile in order to be on the collision triangle is then indicated by $\vec{v}_{Mideal}$ [9]

In this approach, the command angles for the pitch and yaw planes, i.e. γ_m^c and η_m^c, can be generated as follows [1]:

$$\gamma_m^c = \arctan\left[(\Delta z - v_{Tz}\Delta t)/\left(\varsigma_x \cos(\eta_m) + \varsigma_y \sin(\eta_m)\right)\right] \quad (20)$$

$$\eta_m^c = \arctan\left[(v_{Ty}\Delta t - \Delta y)/(v_{Tx}\Delta t - \Delta x)\right] \quad (21)$$

Here, for i=x, y, z and j=M, T; $\varsigma_x = v_{Tx}\Delta t - \Delta x$, $\varsigma_y = v_{Ty}\Delta t - \Delta y$, and $\Delta i = i_M - i_T$ as x, y, and z show the position components on the Earth-fixed frame. Also, Δt denotes the duration required for the missile to attain the predicted intercept point from its current position, and is a function of the position and velocity components of the missile and target.

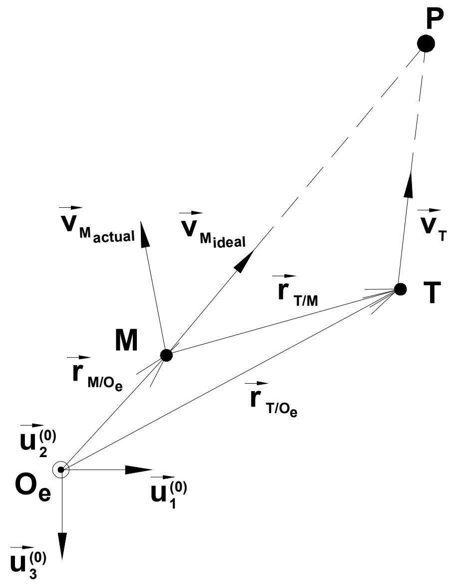

Figure 2. Linear Homing Guidance law geometry.

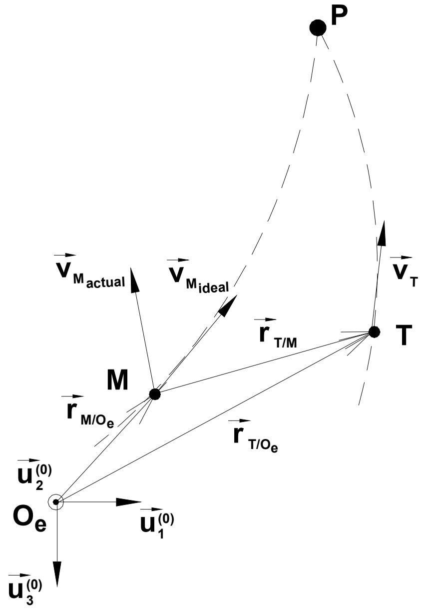

Figure 3. Parabolic Homing Guidance law geometry.

4.2. Parabolic Homing Guidance Law

In the PHG law, the missile is driven to the predicted intercept point with the target by means of a parabolic trajectory as given in Figure 3. In order to keep the missile on the planned trajectory, the necessary guidance commands are generated in the form of lateral acceleration components in the following manner [1]:

$$a_p^c = -d_1 \sin(\eta_m) + d_2 \cos(\eta_m) \quad (22)$$

$$a_y^c = (d_1 + d_2)\sin(\gamma_m) + d_3\cos(\gamma_m) \qquad (23)$$

As a_{Ti} represents the component of the target acceleration on axis i (i=x, y, z) and γ_m and η_m denote the flight path angles in the pitch and yaw planes, the following definitions are made in equations (22) and (23). Here, Δt is a function of the position and velocity components of the missile and target.

$$d_1 = 2\left[\left(v_{Tx} - v_M\cos(\eta_m)\cos(\gamma_m)\right)/\Delta t - \left(\Delta x/\Delta t^2\right)\right] + a_{Tx}$$

$$d_2 = 2\left[\left(v_{Ty} - v_M\sin(\eta_m)\cos(\gamma_m)\right)/\Delta t - \left(\Delta y/\Delta t^2\right)\right] + a_{Ty}$$

$$d_3 = 2\left[\left(v_{Tz} + v_M\sin(\gamma_m)\right)/\Delta t - \left(\Delta z/\Delta t^2\right)\right] + a_{Tz}$$

4.3. Proportional Navigation Guidance Law

Regarding the guidance laws handled in this work, the most famous one is the PNG law. The fame of this method comes from its simplification and ease of implementation. Here, this approach is also accounted in order to compare the performance characteristics of the LHG and PHG laws.

According to the PNG law, the acceleration commands can be calculated for the pitch and yaw control systems in the following manner [1], [10]:

$$a_p^c = -N_p\, v_M\, \dot{\lambda}_p\, \cos(\lambda_y - \eta_m) \qquad (24)$$

$$a_y^c = N_y\, v_M\left[\dot{\lambda}_y\cos(\gamma_m) - \dot{\lambda}_p\sin(\gamma_m)\sin(\lambda_y - \eta_m)\right] \qquad (25)$$

In equations (24) and (25), as p and y stand for the pitch and yaw planes respectively, a_p^c and a_y^c denote the reference, or command, acceleration signals, N_p and N_y represent the effective navigation ratios, and λ_p and λ_y show the line-of-sight angle components.

5. MISSILE CONTROL SYSTEM

The missile control system designed to realize the command signals generated by the considered guidance law consists of the controller, control actuation system, gyroscopes, accelerometers, and plant. In the computer simulations, the plant is directly described by the missile equations of motion rather than the linearized transfer functions so as to model the nonlinear dynamic behavior of the missile correctly. Moreover, the dynamics of the gyroscopes and accelerometers are neglected because their operating frequency values are very high (around 110 Hz) compared to the missile control system bandwidth. The bandwidth of the control actuation system is selected to be 20 Hz such that it does not affect the control system dynamics whose bandwidth is assigned to be 5 Hz. Also, the motions of the control fins are limited by ±20°.

5.1. Angle Autopilot

In order to convert the angle commands produced by the LHG law into physical motions, an angle control system is constructed based on the state-feedback algorithm. In this control system, the integral of the error between the flight path angle command and actual flight path angle value is assigned as the additional state variable. As similar to that in the yaw plane, the angle control system in the pitch plane is given by the block diagram in Figure 4.

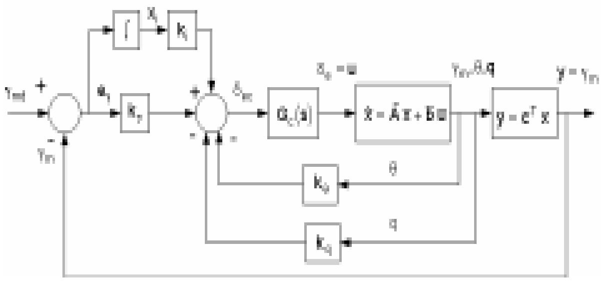

Figure 4. Angle autopilot for the pitch plane.

In the computer simulations, the autopilot gains are continuously updated depending on the current values of the M_∞, magnitude of the missile velocity vector, axial velocity component, pitch/yaw rate, and dynamic pressure. In order to get the corresponding autopilot gains, the closed-loop transfer functions derived from the linearized pitch and yaw plane equations of motion are determined in the following manner:

$$\frac{\gamma_m(s)}{\gamma_{md}(s)} = \frac{n_{\gamma 3}s^3 + n_{\gamma 2}s^2 + n_{\gamma 1}s + 1}{d_{\gamma 4}s^4 + d_{\gamma 3}s^3 + d_{\gamma 2}s^2 + d_{\gamma 1}s + 1} \qquad (26)$$

$$\frac{\eta_m(s)}{\eta_{md}(s)} = \frac{n_{\eta 3}s^3 + n_{\eta 2}s^2 + n_{\eta 1}s + 1}{d_{\eta 4}s^4 + d_{\eta 3}s^3 + d_{\eta 2}s^2 + d_{\eta 1}s + 1} \qquad (27)$$

In equations (26) and (27), as $\gamma_{md} = \gamma_m^c$ and $\eta_{md} = \eta_m^c$, the coefficients $n_{\gamma 3}$, $n_{\gamma 2}$, $n_{\gamma 1}$, $d_{\gamma 4}$, $d_{\gamma 3}$, $d_{\gamma 2}$, $d_{\gamma 1}$, $n_{\eta 3}$, $n_{\eta 2}$, $n_{\eta 1}$, $d_{\eta 4}$, $d_{\eta 3}$, $d_{\eta 2}$, and $d_{\eta 1}$ are functions of the diameter, mass, moment of inertia, and velocity components of the missile as well as the autopilot gains, dynamic pressure, and aerodynamic coefficients.

The autopilot gains are obtained by equating a fourth-order Butterworth polynomial to the characteristic polynomial of each transfer function in equations (26) and (27) in order to make the missile control system stable and to reach the desired bandwidth value, i.e. 5 Hz.

5.2. Acceleration Autopilot

The pitch and yaw acceleration autopilots are designed to realize the reference acceleration commands dictated by the PHG and PNG laws. The pitch control system is shown in Figure 5. Using the yaw equations of motion of the missile, the yaw control system can also be constructed in the same way.

The autopilot acting as the controller in the control system is built such that it makes the error correction according to the proportional plus integral, i.e. PI, control law supplemented by the pitch/yaw rate feedback. Unlike a frozen-gain controller, an adaptive autopilot model is constructed so as to keep the control system stable against varying flight conditions. In this model, the proportional, integral, and pitch/yaw feedback gains (K_p, T_p, and K_q for the pitch autopilot and K_y, T_y, and K_r for the yaw autopilot) are functions of the M_∞, magnitude of the missile velocity vector, axial velocity component, pitch/yaw rate, and dynamic pressure. For this reason, a table involving the aerodynamic stability derivatives within the M_∞ range given above is formed and the control gains are updated depending on the current flight conditions using this table. Furthermore, an anti-windup scheme is added to the control system in order to prevent the miss distance resulted from the windup effect of the integral action in the controller [1].

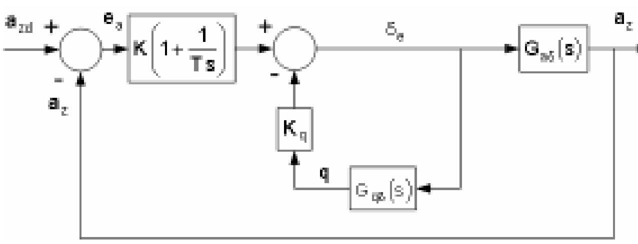

Figure 5. Acceleration autopilot for the pitch plane.

In order to get the corresponding autopilot gains, the closed-loop transfer functions derived from the linearized pitch and yaw plane equations of motion are determined in the following manner:

$$\frac{a_z(s)}{a_{zd}(s)} = \frac{(T_p s+1)(n_{p2} s^2 + n_{p1} s + 1)}{a_{p3} s^3 + a_{p2} s^2 + a_{p1} s + 1} \quad (28)$$

$$\frac{a_y(s)}{a_{yd}(s)} = \frac{(T_y s+1)(n_{y2} s^2 + n_{y1} s + 1)}{a_{y3} s^3 + a_{y2} s^2 + a_{y1} s + 1} \quad (29)$$

In equations (28) and (29), as $a_{zd} = a_p^c$ and $a_{yd} = a_y^c$, the terms T_p, n_{p2}, n_{p1}, a_{p3}, a_{p2}, a_{p1}, T_y, n_{y2}, n_{y1}, a_{y3}, a_{y2}, and a_{y1} are functions of the diameter, mass, moment of inertia, and velocity components of the missile as well as the autopilot gains, dynamic pressure, and aerodynamic coefficients. The autopilot gains $K_p(K_y)$, $T_p(T_y)$, and $K_q(K_r)$ which guarantee the stability of the control system can be found by equating a third-order Butterworth polynomial in equation (30) to the characteristic polynomial of each transfer function in equations (28) and (29) [1].

$$B(s) = (1/\omega_c^3)s^3 + (2/\omega_c^2)s^2 + (2/\omega_c)s + 1 \quad (30)$$

This way, setting ω_c=31.4 rad/s corresponding to the desired bandwidth value of 5 Hz in equation (30), the coefficients $K_p(K_y)$, $T_p(T_y)$, and $K_q(K_r)$ are obtained.

6. TARGET KINEMATICS

Specifying the normal and tangential acceleration components, i.e. a_T^n and a_T^t, in addition to the initial values of the velocity and flight path angle, i.e. v_{T0} and γ_{t0}, the velocity and flight path angle of the target (v_T and η_t) can be expressed depending on time as follows:

$$v_T(t) = v_{T0} + \int_{t_0}^{t} a_T^t(s)\,ds \quad (31)$$

$$\eta_t(t) = \eta_{t0} + \int_{t_0}^{t} \frac{a_T^n(s)}{v_T(s)}\,ds \quad (32)$$

In equations (31) and (32), t_0 denotes the initiation of the missile-target engagement.

Taking the time integrals of equations (31) and (32), the expressions giving the change of the target position with respect to time can be determined for the specified initial values of the target position in the horizontal plane, i.e. x_{T0} and y_{T0}. Since a surface target is concerned in this study, the elevation of the target is taken to be constant, i.e. $z_T(t) = z_{T0}$.

$$x_T(t) = x_{T0} + \int_{t_0}^{t} v_T(s)\cos(\eta_t(s))\,ds \quad (33)$$

$$y_T(t) = y_{T0} + \int_{t_0}^{t} v_T(s)\sin(\eta_t(s))\,ds \quad (34)$$

7. ENGAGEMENT MODEL

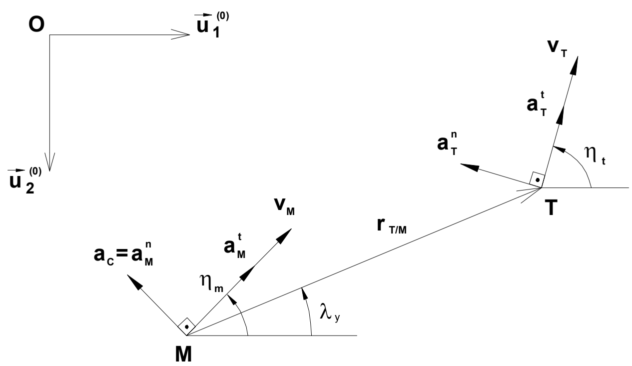

Figure 6. Pitch-plane engagement geometry.

Regarding the missile-target engagement geometry whose pitch-plane representation is schematized in Figure 6, the distance between the missile and target, i.e. $r_{T/M}$, and the line-of-sight angles defined as the angles from $r_{T/M}$ to the pitch and yaw planes, i.e. λ_y and λ_p, can be written in the following fashion:

$$r_{T/M} = \left(\Delta x^2 + \Delta y^2 + \Delta z^2\right)^{1/2} \quad (35)$$

$$\lambda_p = \arctan\left(-\Delta z \cos(\lambda_y)/\Delta x\right) \quad (36)$$

$$\lambda_y = \arctan(\Delta y / \Delta x) \tag{37}$$

In the computer simulations, a strapdown, or body-fixed, seeker model with the field-of-view of ±50° is used [11].

Since a surface target is considered in the study, the total miss distance at the end of the missile-target engagement, i.e. dmiss at $t=t_F$ can be calculated from the following formula just as the vertical component of $r_{T/M}$ becomes zero, i.e. $\Delta z=0$.

$$d_{miss} = \left(\Delta x^2(t_F) + \Delta y^2(t_F)\right)^{1/2} \tag{38}$$

8. COMPUTER SIMULATIONS

Using the entire guidance and control model, the performances of the proposed guidance methods are evaluated for the different values of the missile initial heading error and normal component of the target accelerations. The relevant computer simulations are carried out in the MATLAB® SIMULINK® environment. The terminal miss distance, engagement time, maximum acceleration requirement, and total energy consumption are chosen as the performance criteria. In this extent, it is assumed that the target has a motion of constant velocity, i.e. the motion with zero tangential acceleration component, and hence only the normal, or lateral, acceleration component of the target is taken into account. In the computer simulations with $N_{py}=N_p=3$, initial heading errors of 0 and −20°, and target lateral acceleration level of 0 and 0.5g ($g=9.81\ m/s^2$), the results obtained from the computer simulations under the specified initial conditions are presented in Table 1. In the simulations, the lateral acceleration limit the missile can endure is taken to be ±30g.

In the simulations, the total energy consumption of the missile (E_{tot}) is calculated for each situation using the next formula.

$$E_{tot} = \int_{t_0}^{t_F} P_{ins}\, dt \tag{39}$$

where $P_{ins} = |Y \cdot v| + |Z \cdot w| + |L_1 \cdot p| + |M \cdot q| + |N \cdot r|$ is defined as the instantaneous power consumption.

Table 1. Simulation results.

Initial Heading Error (°)	Target Lateral Acceleration (g)	Guidance Law	Terminal Miss Distance (m)	Missile-Target Engagement Time (s)	Maximum Acceleration Requirement (g)	Total Energy Consumption (kJ)
0	0	LHG*	2.435	3.052	57.154	2.755
		PHG**	7.645	3.040	12.928	33.514
		PNG***	4.840	3.047	2.951	12.257
0	0.5	LHG	3.430	3.039	57.154	2.699
		PHG	7.171	3.031	11.936	29.677
		PNG	4.632	3.038	3.084	13.415
-20	0	LHG	3.205	3.049	942.950	172.717
		PHG	3.473	3.299	12.109	228.143
		PNG	5.578	3.288	16.528	217.395
-20	0.5	LHG	3.325	3.039	942.950	172.852
		PHG	3.387	3.325	12.702	263.109
		PNG	5.597	3.306	16.528	239.068

*LHG: Linear Homing Guidance **PHG: Parabolic Homing Guidance, and *** PNG: Proportional Navigation Guidance

9. DISCUSSION AND CONCLUSION

Looking at the results in Table 1 carefully, it is seen that the terminal miss distance and total energy consumption values attained by the LHG law are the lowest among those obtained for the other guidance laws for all the situations. Moreover, the PNG law seems to be superior to the PHG in terms of the total energy consumption and terminal miss distance with zero initial heading error. On the other hand, the results of the PHG law are better than those of the PNG law in the case of nonzero initial heading error. However, since the LHG tries to put the missile velocity vector upon the collision triangle at the beginning of the engagement, the initial acceleration requirement of the LHG law is the highest. As seen from Table 1, these demands can not be satisfied by the missile with the specified acceleration limit. One of the remedies to overcome this problem is to make the bandwidth of the missile control system varying in accordance with the heading error value [1].

In the sense of maximum acceleration requirements, the best results are reached with the PNG law when the initial heading error is zero. Conversely, the PHG demands the smallest acceleration in the case of nonzero initial heading error condition. The missile-target engagement time values are nearly equal for all the situations considered. Also, the missile trajectory imposed by the LHG law is more flat than the trajectories of the other two [1]. This, in fact, results in very low energy consumption values.

Another interesting note from the results in Table 1 is that some of the values obtained for the cases in which at least either of the initial heading error and target lateral acceleration is different from zero seem to be better than the values attained with zero initial heading error and no target lateral acceleration situation. That means the nonzero conditions may help the missile hit the target in certain circumstances.

Consequently, as long as the acceleration requirements are satisfied, the LHG law yields better results than the PHG and PNG laws.

REFERENCES

[1] Özkan, B., “Dynamic Modeling, Guidance, and Control of Homing Missiles”, Ph.D. Thesis, ***Middle East Technical University Graduate School of Natural and Applied Sciences***, Ankara, Turkey (2005).

[2] Zarchan, P., “Tactical and Strategic Missile Guidance”, 2nd Edition, ***Progress in Astronautics and Aeronautics***, USA (1994).

[3] Özkan, B., Özgören, M.K., Mahmutyazıcıoğlu, G., “Comparison of the several guidance methods applicable to the laser guided missiles (in Turkish)”, ***12th National Machine Theory Symposium***, Kayseri, Turkey (2005).

[4] Özkan, B., Özgören, M.K., Mahmutyazıcıoğlu, G., “Comparison of the linear homing and proportional navigation guidance laws for the homing missiles (in Turkish)”, ***13th National Machine Theory Symposium***, Sivas, Turkey (2007).

[5] Gurfil, P., Jodorkovsky, M., Guelman, M., “Neoclassical guidance for homing missiles”, ***Journal of Guidance, Control and Dynamics***, 24(3): 452-459 (2001).

[6] Acar, Ş.U., “Trajectory Tracking by Means of Homing Guidance Methods”, M.Sc. Thesis, ***Middle East Technical University Graduate School of Natural and Applied Sciences***, Ankara, Turkey (1996).

[7] Tanrıkulu, Ö., “Non-Linear Flight Dynamics of Unguided Missiles”, Ph.D. Thesis, ***Middle East Technical University Graduate School of Natural and Applied Sciences***, Ankara, Turkey (1999).

[8] Blakelock, J.H., “Automatic Control of Aircraft and Missiles”, ***John Wiley & Sons Inc.***, USA (1965).

[9] Özkan, B., Özgören, M.K., Mahmutyazıcıoğlu, G., “Implementation of linear homing guidance law on a two-part homing missile”, ***17th IFAC World Congress***, Seoul, Republic of Korea (2008).

[10] Özkan, B., Özgören, M.K., Mahmutyazıcıoğlu, G., “Guidance and control of two-part homing missiles using the proportional navigation guidance law”, ***AIAA Guidance, Navigation, and Control Conference and Exhibit***, Honolulu, Hawaii, USA (2008).

[11] “Laser Seeker System Workshop”, Martin Marietta Training Notes, ***Martin Marietta Inc.*** (1993).